IEEE Access
Multidisciplinary | Rapid Review | Open Access Journal

Received October 13, 2020, accepted November 3, 2020, date of publication November 10, 2020,
date of current version November 20, 2020.

Digital Object Identifier 10.1109/ACCESS.2020.3037157

A Method for Retrieving Wave Parameters From Synthetic X-Band Marine Radar Images

YANBO WEI[1], YAN ZHENG[2], AND ZHIZHONG LU[2]
[1]College of Physical and Electronic Information, Luoyang Normal University, Luoyang 471934, China
[2]College of Intelligent Systems Science and Engineering, Harbin Engineering University, Harbin 150001, China

Corresponding author: Zhizhong Lu (luzhizhong@hrbeu.edu.cn)

This work was supported in part by the National Natural Science Foundation of China under Grant 41901297.

ABSTRACT The research on retrieving wave parameters from X-band marine radar images based on the spectral analysis method is investigated in this paper. Since the sea wave field is not always homogeneous and stationary in the spatial and temporal domain, especially in the coastal shallow water area, the two-dimensional continuous wavelet transform (2D CWT) is currently utilized to retrieve wave spectrum and wave parameters for improving the inversion accuracy. Although the wavelet is concentrated around the given wavenumber, the CWT of the original image is spread out over a region. By deeply investigating the CWT and its application on radar image, a novel method based on the synchrosqueezed wavelet transform (SWT) is proposed to effectively extract wave parameters from the radar images. The effectiveness of the proposed algorithm is verified based on the simulated radar image. The experimental results demonstrate that the proposed SWT method has better performance than the traditional three-dimensional fast Fourier transform (3D FFT) method and the wavelet-based method for retrieving wave height. The performance of retrieving wave direction and wave period is close to that of both the 3D FFT-based method and the CWT-based method.

INDEX TERMS Marine radar images, synchrosqueezed wavelet transform, wave parameters.

I. INTRODUCTION

Ocean wave is an important component of ocean physical elements. It is highly random and irregular in both time and space domains, which makes it difficult for us to understand and measure the evolution law of ocean parameters [1], [2]. Thus, it is of great significance to understand the wave and its related characteristics in the activities of ocean exploitation [3].

X-band marine radar has a very important guiding significance for the safety of ports and maritime operations. Since the X-band marine radar has the characteristics of low cost, easy operation, real-time and convenience, it is usually used for ship navigation. Besides, the sea clutter contained in marine radar images is rich and has high temporal and spatial resolution. In recent years, X-band marine marine radar is utilized to real-time measure and monitor large-scale sea wave information, such as wave directions, significant wave height. Currently, the research on retrieving wave parameters from X-band marine radar images is one of the hot issues in the field of ocean remote sensing [4]–[6].

The associate editor coordinating the review of this manuscript and approving it for publication was Haiyong Zheng.

The remote measurement of sea waves by using marine radar is based on the light and dark stripes in the radar image, which is called sea clutter. It is formed by the backscattering of radar-emitted electromagnetic waves grazing onto the sea surface. Due to the restriction of the installation height of radar antenna, the main beam of electromagnetic wave transmitted by X-band marine radar is almost parallel to the sea surface when it grazes into the sea surface. Therefore, the X-band marine radar images are mainly affected by shadowing modulation [7]–[9]. The wave parameters are commonly retrieved from the radar image without rainfall interference. However, the collected X-band radar images usually contain rainfall interference noise. The rainfall interference will lead to reducing the quality of the radar image and the reliability of the retrieving results [10], [11]. Thus, it is necessary to detect rainfall in radar images before retrieving wave parameters. Currently and commonly, the spectral analysis method is the mainly method for extracting wave parameters from the collected X-band radar images.

For the traditional spectral analysis method, the image spectrum is obtained by using a three-dimensional fast Fourier transform (3D FFT) on the radar image sequence [12], [13]. Then, the dispersion bandpass filter is utilized to extract the wave spectrum from the obtained image spectrum.

The signal-to-noise ratio (SNR) of the wave signal is calculated based on the wave spectrum. Finally, the linear empirical relationship between the significant wave height and the root mean square of the SNR is used to estimate the significant wave height. In addition, the wave direction and wave period can be achieved from the obtained directional spectrum and frequency spectrum, respectively.

Since the wave field is not always stationary and homogeneous, a quadratic polynomial-based modulation transfer function (MTF) was proposed to calibrate the image spectrum [14]. And the validity of the algorithm was verified by the data collected by vertical polarization radar. The experiments show that the retrieved wave parameters based on the proposed novel quadratic polynomial-based MTF have higher accuracy than that of using the traditional MTF. The effect of the radar field of view (FOV) on wave spectrum and wave parameters was demonstrated [15]. For the sake of removing the dependency of wave parameters on azimuth and range, an empirical method for improving inversion accuracy was investigated. By utilizing the cross-spectral analysis of the radar image sequence, a method for extracting wave direction from X-band marine radar images in the non-homogeneous coastal area is developed in [16].

Nowadays, the one-dimensional continuous wavelet transform (1D CWT) was applied for analyzing the non-stationary signals. For the analysis of ocean waves, the CWT was utilized to analyze the acceleration signals acquired of the wave buoy [17]. Both the wavelet sampling and the scale selection were described [18]. Meanwhile, the Morlet wavelet was used to analyze the non-stationary signals. In the experiment, the validity of 1D CWT was demonstrated. In [19], the two-dimensional curvelet transform (2D CT) was utilized to extract wave spectra and wave direction from X-band marine radar images. Also, the 180° direction ambiguity was removed by using the cross-correlation coefficients. The experimental results show that the retrieved wave direction based on the 2D CT method has better accuracy than that of the traditional 3D FFT method.

Because of the complex submarine topography in nearshore area and the influence of coastline and island on wave reflection and diffraction, the hypothesis of homogeneity of the wave field is not always satisfied. To solve this problem, the CWT was introduced into the marine radar image processing. Currently, the 2D CWT instead of the traditional 3D FFT is applied to retrieve wave spectra from the X-band marine radar images [20]–[22]. The effectiveness of the 2D CWT is verified based on the collected radar data. The retrieving method based on the CWT can better reflect the non-stationary characteristics of wave in the shallow sea and other areas which is vulnerable to the influence of seabed topography. Compared with the reference in-situ buoy, the performance of 2D CWT is better than that of the traditional 3D FFT method. For the CWT, the detailed analysis and configuration of the Morlet wavelet were described in [22], [23]. Based on the simulated radar image and the horizontally polarized radar data, a sophisticated program was illuminated to retrieve wave spectrum and wave parameters [23]. The self-adaptive 2D CWT method, which could adaptively choose the dilation factor, is proposed for retrieving the wave parameters [24]. By using the authentic radar data, the experimental results show that the retrieved wave parameters by utilizing the self-adaptive 2D CWT method agree well with the buoy records. Based on the localized 2D CWT, an improved method for retrieving water depth was proposed for nearshore area from the simulated and collected X-band radar images [25]. The experimental results demonstrate that the proposed method based on the 2D CWT has a good performance compared to the reference value.

For the non-homogeneous sea wave area, the accuracy of the wave spectra and wave parameters extracted based on the 2D CWT method is better than that of the traditional 3D FFT method. However, the CWT of the original signal is spread out over a region around the given wavenumber, even though the wavelet is concentrated around the given wavenumber [26]. To solve this problem, by deeply investigating the characteristic of the CWT, the SWT is utilized to analyze harmonic signal [27]. The synchrosqueezing was carried out based on the Morlet wavelet transform, and the effectiveness of the SWT is certified by using the synthesized marine radar image. In [28], the 2D synchrosqueezed transform is utilized to analyze the crystal image. The experimental results show that the 2D synchrosqueezed transform is an efficient tool for multiscale analysis and can extract reliable properties of the crystal image. In this paper, based on the synchrosqueezed wavelet theory, a novel SWT method for extracting wave information from the marine radar images is proposed.

Our primary goal is to develop a novel spectral analysis algorithm, which could solve the problem that the obtained image spectrum based on the CWT on the original radar image is spread out over a region around the given scale. Due to the reallocation characteristic of the SWT by reallocating the scale spectral value of CWT to a different wavenumber position, the 2D SWT instead of the 2D CWT is utilized to extract wave spectra from the radar images. To demonstrate the effectiveness, the SWT and its application for retrieving the wave parameters from the synthetic marine radar image are illustrated in this paper. This paper is structured as follows: Section II presents the basic 2D CWT method and its application for retrieving wavenumber image spectrum from the X-band marine radar images. In Section III, the theoretical analysis and the novel synchrosqueezed wavelet-based algorithm for retrieving wavenumber image spectrum and wave parameters from the radar images are developed. Based on the radar images simulated, the effectiveness of the proposed method is investigated in Section IV. Finally, the conclusion is summarized in Section V.

II. 2D CWT AND ITS APPLICATION FOR RETRIEVING WAVENUMBER IMAGE SPECTRUM

In this section, the Morlet wavelet is briefly reviewed and the application of 2D CWT for retrieving sea wave spectrum from X-band marine radar images is introduced.

A. THE MORLET WAVELET

Before applying the 2D CWT to extract the directional frequency spectrum and the wave parameters, a directional mother wavelet function is required to be specified. Since the well-known Morlet wavelet function is chosen for marine radar image analysis in [20], [24], here we continue to utilize it. The expression of the simplified 2D Morlet wavelet used in the spatial domain for marine radar imaging processing is given as

$$\Psi(\vec{\gamma}) = e^{i\vec{k}_0\cdot\vec{\gamma}}e^{-|\vec{\gamma}|^2/2} \tag{1}$$

where the peak wavenumber of the mother wavelet in the non-dimensional Fourier space $\vec{k}_0 = (6, 0)$ is adopted to analyze the radar image; $\vec{\gamma}$ is the pixel coordinate of the radar image. The Fourier transform of the Morlet mother wavelet is

$$\hat{\Psi}(\vec{k}) = e^{-0.5|\vec{k}-\vec{k}_0|^2} \tag{2}$$

where $\vec{k}$ is the wavenumber.

B. 2D CWT FOR RADAR IMAGE PROCESSING

In order to apply the CWT to analyze dimensional radar images, the process of both discretization and sampling is required. The 2D CWT in dimensional space can be written discretely as [20], [24]

$$\begin{aligned} &W(b_{x_u}, b_{y_v}, \theta_m, a_n) \\ &= C_\Psi^{-0.5} a_n^{-1} \\ &\quad \cdot \sum_{p=1}^{N_x}\sum_{q=1}^{N_y} \Psi^*[a_n^{-1} r_{-\theta_m}(x_p - b_{x_u}, y_q - b_{y_q})] s(x_p, y_q)\Delta x \Delta y \end{aligned} \tag{3}$$

in which C_Ψ is a constant and satisfies the admissibility condition; $s(x_p, y_q)$ denotes the selected radar image; x_p and y_q are the sampling positions in the x and y directions of the radar image, respectively; N_x and N_y are the total sampling numbers in the x and y directions, respectively; Ψ^* is the complex conjugate of an appropriately chosen mother wavelet function Ψ; Δx and Δy are the sampling resolutions of radar image in the x and y directions; b_{x_u}, b_{y_v} and a_n denote the discrete variables of shifting factor and scaling factor. The rotation matrix $r_{-\theta_m}$, which denotes the rotation of the wavelet in spatial domain, is expressed as

$$r_{-\theta_m} = \begin{pmatrix} \cos\theta_m & \sin\theta_m \\ -\sin\theta_m & \cos\theta_m \end{pmatrix} \tag{4}$$

where the discrete variable θ_m is the rotation factor and $0 \le \theta_m < 2\pi$.

Due to the computationally intensive in Eq.(3), it is vital to reduce the algorithm execution time. By Plancherel's theorem, the 2D CWT in Eq.(3) can be rewritten in the Fourier space as [20], [24]

$$\begin{aligned} &W(b_{x_u}, b_{y_v}, \theta_m, a_n) \\ &= C_\Psi^{-0.5} a_n \sum_{p=1}^{N_{k'_x}}\sum_{q=1}^{N_{k'_y}} e^{i(b_{x_u}k'_{x_p} + b_{y_v}k'_{y_q})} \\ &\quad \cdot \hat{\Psi}^*[a_n r_{-\theta_m}(k'_{x_p}, k'_{y_q})]\hat{s}(k'_{x_p}, k'_{y_q})\Delta k'_x \Delta k'_y \end{aligned} \tag{5}$$

where $\hat{s}$ is the FT of the echo intensity of radar image s. $N_{k'_x} = N_x$ and $N_{k'_y} = N_y$ are the total numbers of the sampled wavenumber in the x and y directions, respectively. $\vec{k}' = (k'_x, k'_y)$, which is derived from the mapping of the wavenumber $\vec{k} = (k_x, k_y)$ in the non-dimensional space, is the wavenumber in the dimensional space, where $k'_x \in [-\frac{N_x}{2}\Delta k'_x, \frac{N_x}{2}\Delta k'_x]$ and $k'_y \in [-\frac{N_x}{2}\Delta k'_y, \frac{N_x}{2}\Delta k'_y]$. $N_{k'_x} = N_x$ and $N_{k'_y} = N_y$ are the total numbers of the sampled wavenumber in the x and y directions, respectively. $\Delta k'_x$ and $\Delta k'_y$, which are the wavenumber resolution in the dimensional wavenumber domain, are denoted as

$$\Delta k'_x = \frac{2\pi}{N_x \Delta x} \tag{6}$$

$$\Delta k'_y = \frac{2\pi}{N_y \Delta y} \tag{7}$$

As mentioned in [20], [24], the relationship between peak wavenumber $\vec{k}'$ in dimensional space and the peak wavenumber $\vec{k}_0$ of the Morlet wavelet function in the non-dimensional Fourier space is given as

$$\vec{k}_0 = a_n r_{-\theta_m}(\vec{k}') \tag{8}$$

It reveals that the wavenumber $\vec{k}'$ can be achieved from scaling parameter a_n and rotation parameter $r_{-\theta_m}$. Therefore, the obtained image spectrum $W(\vec{b}, \theta, a)$ after taking 2D CWT could be expressed as $W(b_{x_u}, b_{y_v}, \vec{k}')$ which denotes the spectrum $W(\vec{k}')$ at spatial location (b_{x_u}, b_{y_v}). Once the shift parameter $\vec{b}$ is fixed, the 2D wavenumber image spectrum $W(\vec{k}')$, which is the spectrum information extracted from the inhomogeneous radar image, can be obtained. Thus, we have

$$W(\vec{b}, \theta, a) \xrightarrow{CWT} W(b_{x_u}, b_{y_v}, \vec{k}') \xrightarrow{b_{x_u}, b_{y_v}} W(\vec{k}') \tag{9}$$

III. THE PROPOSED METHOD BASED ON THE SYNCHROSQUEEZED WAVELET TRANSFORM FOR RETRIEVING WAVE PARAMETERS

In this section, the SWT and its application for retrieving wave information are illustrated. A flowchart for retrieving the sea wave parameters based on the proposed SWT method is presented in Fig. 1. Now we illustrate the detailed description of the method for retrieving wave parameters from marine radar images.

A. THE NOVEL SWT

Since the SWT is analyzed on the basis of CWT, it is necessary to carry out the CWT on the radar image analysis area to obtain the image wavenumber spectrum $W(\vec{b}, \theta, a)$ including translation, scale and direction parameters. After taking the CWT on the radar image, the image spectrum $W(\vec{b}, \theta, a)$ should concentrate on the specified scale position [26], [27]. However, it spreads out over the region on the scale plane. Thus, an undesired error may introduce to the wavenumber spectrum $W(\vec{k}')$ obtained by the 2D CWT. Fortunately,

the researchers recently found that the oscillatory behavior $e^{i(b_{x_u}k'_{xp}+b_{y_v}k'_{yq})}$ of the CWT in position $\vec{b}$ points to the original the wavenumber k'_{x_p} and k'_{y_q}, even though $W(\vec{b},\theta,a)$ is spread out. For any $(\vec{b},\theta,a)$ for which 2D CWT $W(\vec{b},\theta,a)\neq 0$ in Eq.(5), the wavenumber estimation $\vec{k}'(\vec{b},\theta,a)$ for the radar images is given as

$$\vec{k}'(\vec{b},\theta,a)=\frac{\nabla_{\vec{b}}W(\vec{b},\theta,a)}{iW(\vec{b},\theta,a)} \tag{10}$$

where the symbol ∇ denotes the gradient of image spectrum $W(\vec{b},\theta,a)$ in the position vector $\vec{b}$. The symbol i is the imaginary unit. In a synchrosqueezing operation, the information from the space-scale plane $(\vec{b},\theta,a)$ is transferred to the space-wavenumber plane $(\vec{b},\vec{k}(\theta,a))$, which is different to the scale and rotation transform of the Morlet mother wavelet.

As mentioned in the introduction, here we use the 2D SWT to extract and analyze the wavenumber image spectrum from the synthetic radar images. The wavelet transform $W(\vec{b},\theta,a)$ is computed only at discrete values (θ_m,a_n), with $\theta_m-\theta_{m-1}=(\Delta\theta)_m$ and $a_n-a_{n-1}=(\Delta a)_n$, and its synchrosqueezed transform $T_s(\vec{b},\vec{k}')$ is likewise determined only at the centers (k'_{x_w},k'_{y_l}) of the successive bins $[k'_{x_w}-\frac{1}{2}\Delta k'_x,k'_{x_w}+\frac{1}{2}\Delta k'_x]$ and $[k'_{y_l}-\frac{1}{2}\Delta k'_y,k'_{y_l}+\frac{1}{2}\Delta k'_y]$, with $k'_{x_w}-k'_{x_{w-1}}=(\Delta k')_x$ and $k'_{y_l}-k'_{y_{l-1}}=(\Delta k')_y$ by summing different contributions. Thus, the SWT can be given as

$$\begin{aligned}T(\vec{b},\vec{k}')&=T(\vec{b},k'_{x_w},k'_{y_l})\\&=\sum_{\substack{(\theta_m,a_n):\\|k'_x(\vec{b},\theta_m,a_n)-k'_{x_w}|\le\Delta k'_x/2\\|k'_y(\vec{b},\theta_m,a_n)-k'_{y_l}|\le\Delta k'_y/2}}|W(\vec{b},\theta,a)|^2a_n(\Delta a)_n\\&\quad\cdot(\Delta\theta)_m(\Delta k'_x)^{-1}(\Delta k'_y)^{-1}\end{aligned} \tag{11}$$

Similar to the above 2D CWT, once the shifting factor is specified as $\vec{b}_0$, a 2D SWT wavenumber image spectrum $T(\vec{k}')$ at point $\vec{b}_0$ is determined as

$$W(\vec{b},\theta,a)\xrightarrow{SWT}T(\vec{b},\vec{k}')\xrightarrow{\vec{b}_0}T(\vec{k}') \tag{12}$$

B. WAVELET SAMPLING AND SCALE DETERMINATION

Since the radar image is dimensional and digital, there exists a mapping between the continuous non-dimensional mother wavelet and the radar image [18], [20], [24]. In the non-dimensional space, the length of the mother wavelet equals to $2D$, where D is the cutoff endpoint. In the space domain, assume the N_x and N_y are the sampling numbers in the x and y direction, respectively. Hence, the length of the image in x and y directions is $N_x\triangle x$ m and $N_y\triangle y$ m, respectively. For the x direction, the mappings can be given as

$$[-D,D]\leftrightarrow[0,N_x\triangle x] \tag{13}$$

Since the wavenumber is inversely proportional to the length, the wavenumber $\vec{k}'=(k'_{x_p},k'_{y_q})$ in dimensional space can be written as

$$\hat{\Psi}(k)=\hat{\Psi}(\frac{N_x\Delta x}{2D}k') \tag{14}$$

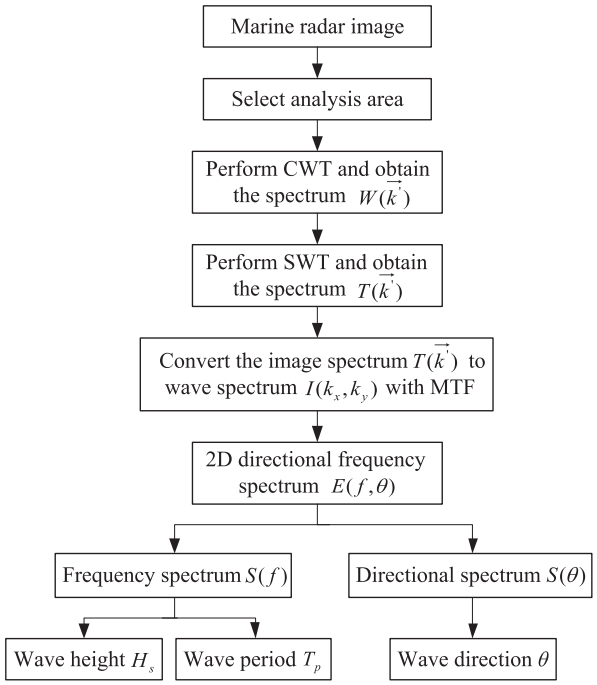

FIGURE 1. The flowchart for retrieving wave parameters based on the proposed SWT method.

Thus, in the dimensional space, the wavelet can be written as

$$\hat{\psi}(a_{x_p}k'_{x_p})=e^{-\left(\frac{a_{x_p}k'_{x_p}N_x\Delta x}{2D}-k_{x_0}\right)^2/2} \tag{15}$$

where is $\hat{\psi}$ the Fourier transform of the Morlet wavelet function in the dimensional space; a_{x_p} denotes the discrete scaling factor; k'_{x_p} is the discrete wavenumber in the dimensional space; k_{x_0} is the peak wavenumber of the wavelet function in x the direction. In dimensional space for the Morlet wavelet, the minimum number of sample pints is written as [18], [20], [24]

$$N_s=\frac{2D}{\pi}(k_{0_x}+\sqrt{-2\ln(\eta)}) \tag{16}$$

where η is the ratio of wavelet decay from the largest peak wavenumber and usually set to the value of 0.01; k_{0_x} is the peak wavenumber in x direction.

It is known that the bandwidth of wavelet decreases with the scaling parameter increases in wavenumber domain. Assume the scaling factor a_n has the form of the geometric progression. Thus we have

$$a_n=M^{n-1},n=1,2,\cdots,N_a\quad M>1 \tag{17}$$

where $n=1$ corresponds to the mother wavelet. The base M is illuminated as

$$M=\frac{k_p}{k_d+k_p} \tag{18}$$

where $k_p=k_{0_x}$ is the peak position of the mother wavelet, k_d is related to the scale resolution χ and is given as

$$k_d=-\sqrt{-2\ln(\chi)} \tag{19}$$

where $\chi \in (0.0, 1.0)$. For ocean wave analysis, the scale resolution $\chi \in [0.9, 0.95]$ is an appropriate range. The larger χ denotes higher wavelet resolution.

By taking into account the convolution end effects of wavelet coefficient, the maximum scale a_{max} is described as [18]

$$a_{max} \leq \frac{N}{3(N_s - 1)} \tag{20}$$

where N is the sample points of the radar images in x or y direction.

C. 2D WAVENUMBER WAVE SPECTRUM

The wavenumber image spectrum is achieved as

$$I(k_x, k_y) = \frac{|T(k'_x, k'_y)|}{L_x \cdot L_y} \tag{21}$$

Since the effect of the radar imaging mechanisms like shadowing and tilt modulation, a difference is observed between the image spectrum $I(k_x, k_y)$ and the wave spectrum $E(k_x, k_y)$. In order to minimize this difference, the empirical MTF is used to convert the wavenumber image spectrum into wave spectrum, which is given as

$$E(k_x, k_y) = |M(k^2)| \cdot I(k_x, k_y) = k^{\mu} \cdot I(k_x, k_y) \tag{22}$$

where μ is the empirical coefficient. Different sea state conditions were considered to generate simulated radar images by applying different theoretical frequency spectra. The empirical coefficient of the MTF is determined by comparing the difference between the theoretical frequency spectra and retrieved image spectra based on the 3D FFT. The empirical coefficient is determined as for the 3D FFT-based method and the CWT-based method [24], [29].

D. RETRIEVING WAVE PARAMETERS

The relationship between wave spectrum $E(k_x, k_y)$ in Cartesian coordinates and wave spectrum $E(k, \theta)$ in polar coordinates is given as [30]

$$E(k, \theta) = E(k_x, k_y) \cdot k \tag{23}$$

where $k = \sqrt{k_x^2 + k_y^2}$ and $\theta = arctan2(k_y, k_x) + 2\pi$, $arctan2(\cdot)$ is the arctangent function. Commonly, the wave spectrum is expressed as directional frequency spectrum

$$E(f, \theta) = E(k, \theta) \cdot \frac{dk}{df} = E(k_x, k_y) k \frac{dk}{df} \tag{24}$$

The 1D frequency spectrum $S(f)$ is obtained by integrating the direction θ of the directional frequency spectrum $E(f, \theta)$. Similarly, the 1D directional spectrum $S(\theta)$ is derived by integrating the directional frequency spectrum $E(f, \theta)$. After obtaining the 1D directional spectrum $S(\theta)$ and 1D frequency spectrum $S(f)$, both the wave peak period $T_p = 1/f_p$ and wave direction θ can be calculated. In addition, the significant wave height estimated H_s for the radar data is described as [24]

$$H_s = 4\sqrt{m_0} = 4\sqrt{\int_{f_{min}}^{f_{max}} S(f) df} \tag{25}$$

where m_0 is the total energy of sea wave; f_{min} and f_{max} are the lower and upper bounds of the integral, respectively. The wave period observed from the X-band marine radar is usually between 5 s and 20 s. Thus, the lower bound $f_{min} = 0.05$ Hz and the upper bound $f_{max} = 0.2$ Hz of the frequency spectrum are determined based on the variation range of the wave period.

IV. EXPERIMENT RESULTS AND ANALYSIS

In this section, we carry out retrieving the wave parameters such as significant wave height, wave period, wave direction based on the simulated radar images to verify the validity of our proposed method. Based on the simulated radar image, the performance of our proposed method is presented by comparing with that of the existing 3D FFT and 2D CWT methods. The detailed experiment results and analysis are illuminated below.

A. SIMULATED RADAR IMAGES AND ANALYSIS

The Joint North Sea Wave Project (JoNSWaP) spectrum is used to produce the wave surface field [21], [29]. And then, shadowing and tilt modulation are taken into account to generate the marine radar images [29]. Here, the location of the selected region from the radar platform is about 300 m. The antenna height is 25 m. The range resolution of the simulated radar image is 7.5 m.

For the 3D FFT method, the coefficient is determined by using the linear relationship between the root mean square of the SNR and the significant wave height. In our experiment, a set of simulated radar images in different sea conditions is used to calculate the calibration coefficient of the linear relationship. The wave height is used to input the JoNSWaP and generate the simulated radar images. Then, the SNR can be retrieved from the simulated radar images. The experimental coefficient of the linear experimental relationship is determined by using the least square fit algorithm.

Based on the CWT and the SWT, a single radar image is often selected for ocean wave parameters inversion. For analyzing the X-band marine radar image, it is necessary to select the analysis region from the X-band marine radar image. In the experiment, the radar image contains 512×512 pixels.

For the spectral analysis, the wavelet parameters and others are given in Table 1. The scale resolution $\chi \in [0.9, 0.95]$ is commonly used to analyze the marine radar images. Since the larger χ denotes higher wavelet resolution, the parameter $\chi = 0.95$ is selected in this paper, in order to achieve better scale resolution and wavenumber resolution. The selection criteria of the parameters for the 2D CWT described in [22], [24] is adopted. After the transform analysis, the directional ambiguity is observed. Based on the single radar to retrieve sea wave parameters, the obtained wave spectrum usually exists the problem of the wave direction ambiguity. When using the JoNSWaP spectrum to generate the sea wave field, the main wave direction θ_m is used to input the directional propagation function. The wave spectrum in the range

TABLE 1. The Wavelet Parameters and Others.

Wavelet Parameters	Value
peak wavenumber k	6
minimum sample points N_s	17
scale resolution χ	0.95
empirical coefficient u	-1.2

between $\theta_m-180°$ and $\theta_m+180°$ can be selected for retrieving wave parameters. By using the input wave direction, the wave direction 180° ambiguity is removed manually during the experiment for further analysis. For the field data, suppose the initial wave direction is determined by manual observation and is defined as the previous wave direction. Since the wave direction of the sea wave filed usually does not change rapidly, the present wave direction can be extracted by choosing the wave direction which is close to the previous wave direction. Then, we update the previous wave direction by using the obtained wave direction. Thus, the wave direction ambiguity can be removed, when the proposed method is applied to the field data.

The comparison of the directional frequency spectrum $S(f,\theta)$, which provides the major energy distribution, is shown in Fig. 2. Fig. 2(a) indicates the directional frequency spectrum simulated which is used to generate radar image. The frequency directional spectra extracted using the 3D FFT method and the 2D CWT method as well as the SWT method are illustrated in Fig. 2(b), Fig. 2(c) and Fig. 2(d), respectively. From Fig. 2, we found that all these methods could extract main wave energy from the radar image. For the 3D FFT method, a dispersion relation bandpass filter is utilized to extract the wave spectrum. Both the CWT and the SWT method could capture the main wave energy and the wave direction compared to the 3D FFT method. In addition, from Fig. 2(d), it can be found that the energy distribution of the spectrum based on the SWT is more concentrated than that of based on the 3D FFT and CWT.

Fig. 3 reveals the normalized 1D frequency spectra derived for the input, the 3D FFT, the CWT, and the SWT. For the peak frequency and the high-frequency part, the extracted 1D spectrum of the 3D FFT method has a bigger deviation from the simulated 1D frequency spectrum compared to that of the CWT method and the SWT method. Meanwhile, It could be found that the extracted peak frequency of the 1D frequency spectrum based on the WT and SWT methods agrees well with that of the input. Unfortunately, for the high-frequency part, the tailor of the spectrum using the SWT method has a bigger deviation than that of the CWT method compared to the simulated 1D frequency spectrum. However, for low-frequency part, the difference between the extracted 1D spectrum of the SWT method and the input frequency spectrum is smaller than that of the CWT method. Moreover, the achieved frequency spectrum for low-frequency part based on the proposed method is most close to the input among the three retrieving methods.

For the 3D FFT-based method, the significant wave height is extracted based on the empirical relationship between the SNR and the significant wave height from the radar image sequence. However, for the CWT-based and the SWT-based retrieving methods, the single radar image is utilized to retrieve the significant wave height. The significant wave height is determined by using the 1D sea wave spectrum based on the Eq.(25). The detailed comparison between the input and the retrieved parameters using the proposed the SWT algorithm as well as the 3D FFT and the CWT methods is shown in Table 2. It is observed clearly that the retrieved wave information using the proposed method is most close to the input parameters among the three retrieving methods. Since the SWT-based method could concentrate the wave energy, the extracted the wave direction and the peak frequency are close to the input value. Also, the extracted significant wave height based on the SWT method has good performance.

TABLE 2. Comparison of the Input and the Retrieved Wave Parameters.

Wave Parameters	Inout	3D FFT	CWT	SWT
dominant wave direction $\theta(°)$	100	90.7	105	101.3
mean wave period T_{01} (s)	11.03	10.36	10.43	11.09
peak frequency T_p (Hz)	0.0907	0.0990	0.0960	0.0914
significant wave height H_s (m)	3.63	3.01	3.54	3.69

B. RESULTS ANALYSIS

Based on the above analysis, it can be found that the SWT-based method could effectively retrieve wave parameters from the simulated marine radar image. To further certify the effectiveness of the proposed method for retrieving sea state parameters, 500 simulated radar image sequences are applied for validation and analysis. For the 3D FFT method, a standard radar image sequence which consists of 32 images and represents a time span of about 75 s is used to calculate the sea state parameters. Because of the time consuming, the wave parameters based on the CWT and the SWT methods are retrieved from a single simulated radar image of the sequence.

The input wave height and the retrieved significant wave height from the simulated radar images are described in Fig. 4. The horizontal and vertical axes denote the time sequence and the significant wave height, respectively. The range of the input wave height becomes from 1 to 6 m. The input of the significant wave height of the JoNSWaP spectrum is represented by the red cross. The black square is the retrieved significant wave height based on the traditional 3D FFT method and the dispersion relation bandpass filter. The green circle and the blue triangle denote the retrieved significant wave height based on the 2D CWT method and the proposed SWT method, respectively. From Fig. 4, it could be observed that all the 3D FFT-based, 2D CWT-based, and the SWT-based methods could effectively extract significant wave height and the retrieved wave height is consistent with that of the input value.

In order to further verify the performance of the retrieving significant wave height, the scatter plots between the input and the retrieved wave height are described in Fig. 5. Fig. 5(a) is the scatter between the input value and the retrieved wave height base on the 3D FFT method. The scatter between

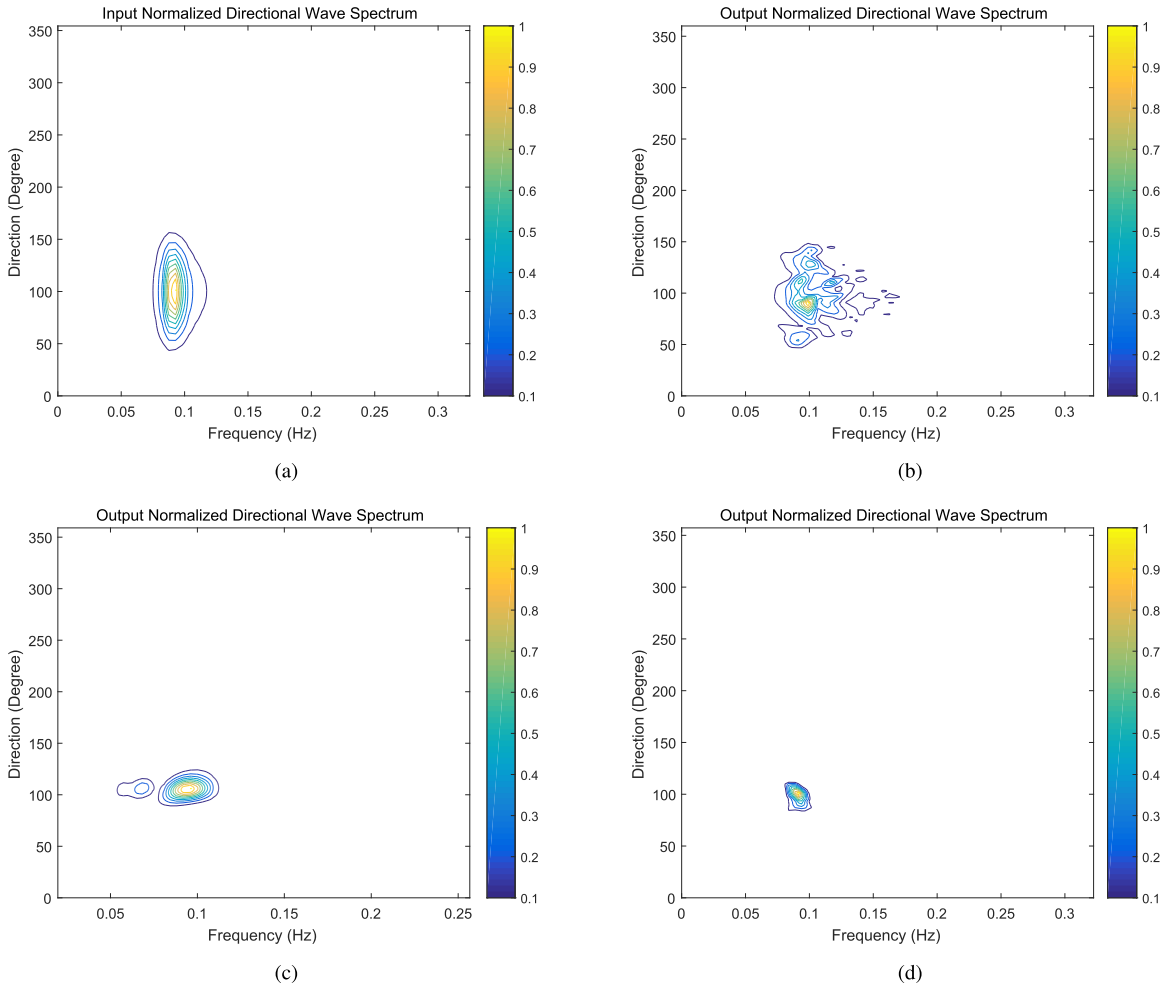

FIGURE 2. Comparison of the results from the simulated data. (a) The input directional frequency spectrum. (b) The 3D FFT derived directional frequency spectrum. (c) The CWT derived directional frequency spectrum. (d) The SWT derived directional frequency spectrum.

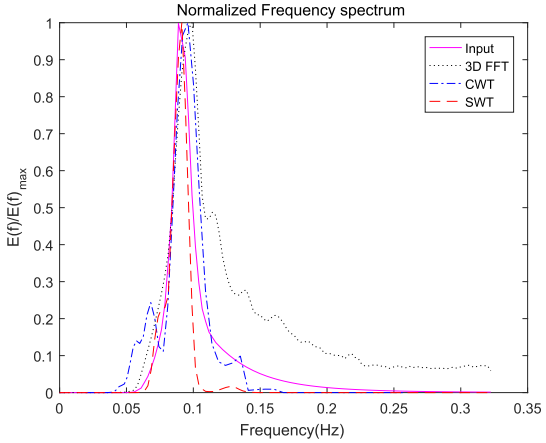

FIGURE 3. The normalized 1D frequency spectrum.

the input value and the retrieved wave height base on the CWT method is described in Fig. 5(b). Fig. 5(c) illustrates the scatter between the input value and the retrieved wave height base on the SWT method. The correlation coefficient between the input and the retrieving results and the root mean square error (RMSE) are used to evaluate the performance of these algorithms. From Fig. 5, it can be found that the correlation coefficients of the Fig. 5(b) and Fig. 5(c) are larger than that of the Fig. 5(a). Also, for the CWT and the SWT method, the RMSE of the wave height is less than that of the 3D FFT method. Although a single simulated image is utilized to retrieve significant wave height, both the CWT and the SWT methods have better performance than that of the 3D FFT method. Moreover, the RMSE of the wave height based on the SWT method is less than that of the CWT method. Thus, it can be found that the SWT method has good performance for retrieving significant wave height.

The scatter plots between the input and the retrieved wave direction are presented in Fig. 6, for the sake of verifying the performance of the retrieving wave direction. Fig. 6(a) is the scatter between the input value and the retrieved wave direction base on the traditional 3D FFT method. The scatter between the input value and the retrieved wave direction base on the CWT method is described in Fig. 6(b). Fig. 6(c) illustrates the scatter between the input value and the retrieved wave direction base on the SWT method.

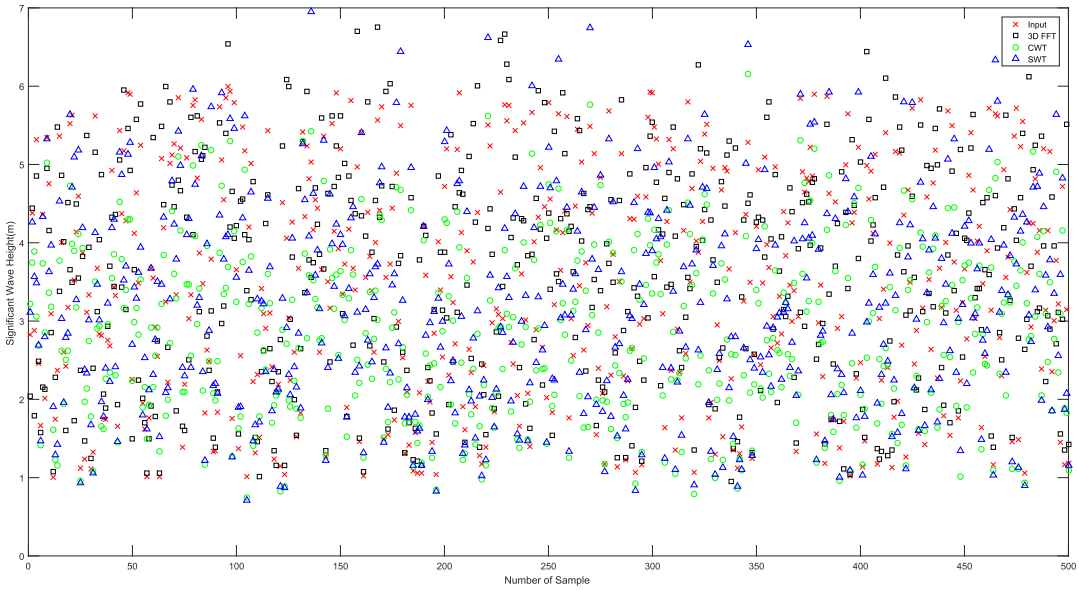

FIGURE 4. The input and the estimated significant wave height.

Compared to Fig. 6(a), it can be found that the correlation coefficients of the retrieving wave direction based on the CWT and the SWT methods also have good performance. Thus, the proposed SWT method can be used to retrieve wave direction from the simulated single image. However, the calculated RMSE based on the CWT and the SWT methods is larger than that of the traditional 3D FFT method. The RMSE of the wave direction based on the SWT method is close to that of the CWT method. Therefore, we have that the performance of the proposed SWT method is close to that of the CWT method for retrieving wave direction. Since the shadowing and the tilt modulation are considered to generate the synthetic radar images, the simulated radar image is not always homogeneous. For the 3D FFT method, the radar image sequence is used to retrieve wave spectrum and wave parameters. The dispersion relationship bandpass filter is used to filter out the non-wave signal from the obtained wave spectrum. Compared to the 3D FFT, the SWT could capture more information for the non-homogeneous sea wave area. However, for the SWT method, the obtained wave spectrum based on a single radar image may contain much non-wave signal. Moreover, the dispersion relationship bandpass filter can not be introduced in the process of retrieving the wave spectrum. Thus, from Fig. 6, we found that the retrieved wave direction based on the SWT method is not close to that of the FFT method and the calculated RMSE is larger than that of the FFT method.

To further demonstrate the effectiveness of the proposed SWT method for retrieving the wave peak period, the scatter plots between the input and the retrieved wave peak period are illuminated in Fig. 7. The scatter between the input value and the retrieved wave peak period base on the traditional 3D FFT method is described in Fig. 7(a). Fig. 7(b) is the scatter between the input value and the retrieved wave peak period base on the 2D CWT method. The scatter between the input value and the retrieved wave peak period base on the proposed SWT method is presented in Fig. 7(c). From Fig. 7, it can be observed that the correlation coefficients of the retrieving wave peak period by using these retrieving methods are close to 1 compared to the reference value. And, a strong correlation with the reference value exists. However, the RMSE of the retrieved wave peak period based on the CWT and the SWT method is larger than that of the 3D FFT method. Although the calculated correlation coefficient based on the proposed SWT method is closet to 1, the RMSE of the wave peak period is the largest among these three retrieving methods.

To solve the problem that the existed 3D FFT-based spectrum analysis method can not accurately extract the wave parameters from the sea wave spectrum in the near-shore area and the 2D CWT-based method spreads out the wave energy over the given scale position, a new retrieving wave information method based on the SWT is proposed in this paper. Based on the above experimental results and analysis, it can be found that the proposed SWT method in this paper could effectively extract wave sea state parameters from the simulated radar images. The experimental results show that the proposed method can improve the inversion accuracy of the significant wave height. However, the retrieving accuracy of the wave peak period and the wave direction is needed to be further improved in the future.

Currently, the sea surface current is commonly retrieved based on the radar image sequence. During the retrieving process, the sea surface current is obtained by using the dispersion relationship bandpass filter. Since the single radar image is utilized to retrieve sea wave parameters for the CWT and SWT methods, the dispersion relationship bandpass filter can not be introduced in the process of inversion. Thus, for

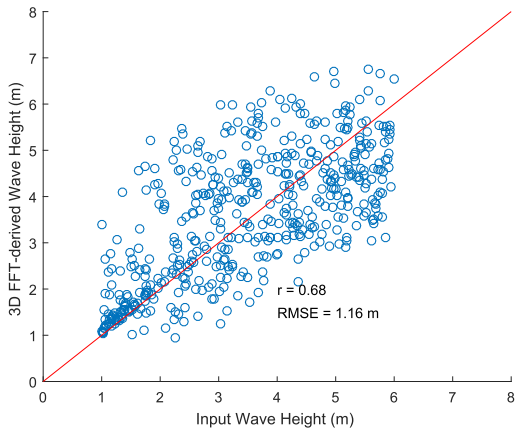

(a)

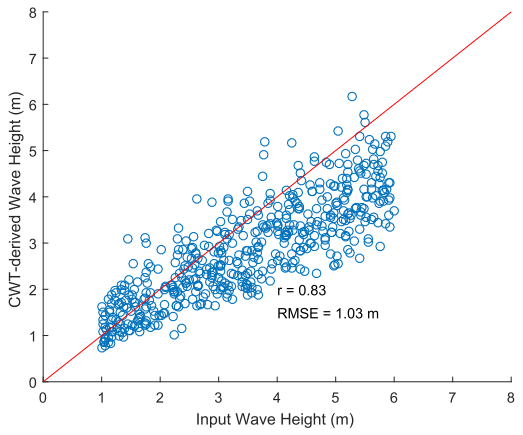

(b)

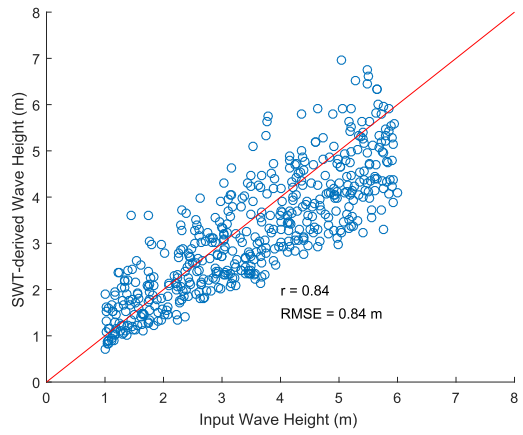

(c)

FIGURE 5. The scatter plots of the significant wave height between the input value and the derived wave height. (a) The 3D FFT-based method; (b) The 2D CWT-based method; (c) The SWT-based method.

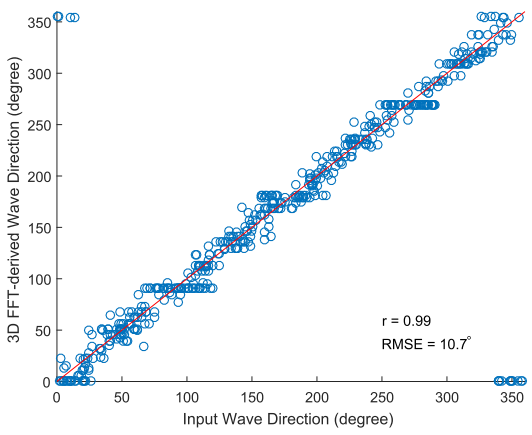

(a)

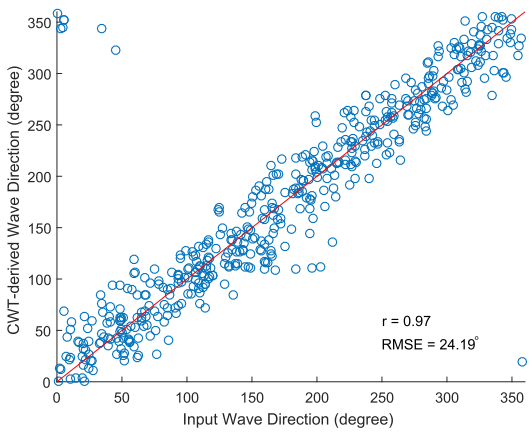

(b)

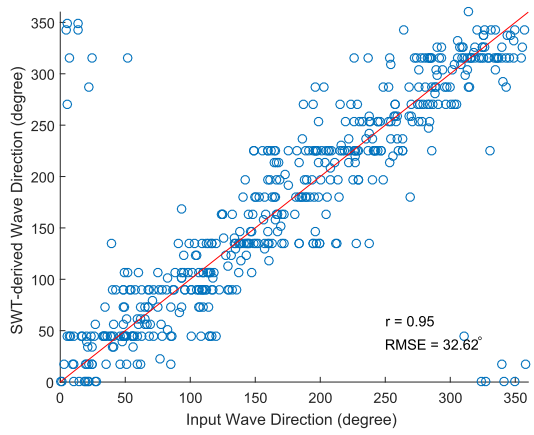

(c)

FIGURE 6. The scatter plots of the wave direction between the input value and the extracted wave direction. (a) The 3D FFT-based method; (b) The 2D CWT-based method; (c) The SWT-based method.

retrieving wave parameters from the single radar image, the effect of the sea surface current on the wave spectrum can not be removed directly. Fortunately, when the sea surface current is small, the effect of the sea surface current on the retrieving wave parameters can be ignored. Therefore, the effect of the surface current is not considered during the experiment in this paper. In the future, the research on the bandpass filter for eliminating the effect of the surface current is demanded based on the field data. Moreover, more experiments are needed to verify the accuracy of the proposed method in different sea conditions.

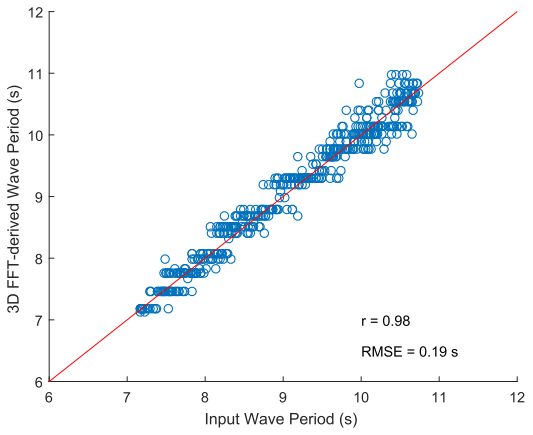

(a)

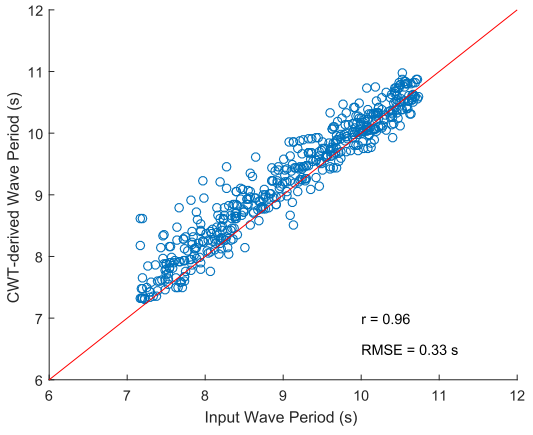

(b)

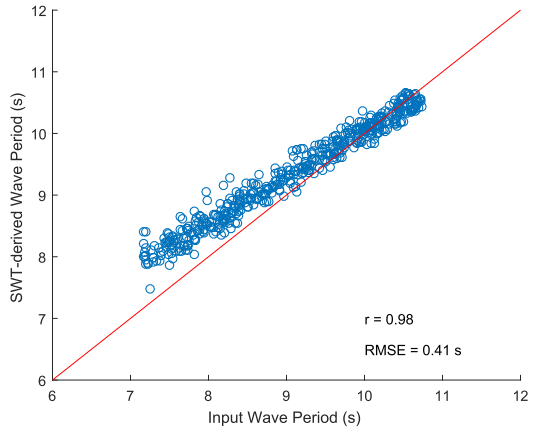

(c)

FIGURE 7. The scatter plots of the wave peak period between the input value and the extracted wave peak period. (a) The 3D FFT-based method; (b) The 2D CWT-based method; (c) The SWT-based method.

V. CONCLUSION

Since the sea wave is a typical non-stationary random process, especially in the coastal area, it is difficult to accurately retrieve wave parameters. In this paper, the spectral analysis method for retrieving sea state information from X-band marine radar images is studied. The CWT instead of the 3D FFT is used to retrieve wave spectrum and wave parameters. However, the CWT of the radar image is spread out over a region around the given wavenumber for the non-homogeneous sea wave area, even though the wavelet is concentrated around the given wavenumber. To solve this problem, by deeply investigating the characteristic of the CWT and its application on radar image, a novel SWT-based method is carried out to extract wave parameters from the marine radar images. The detailed analysis and derivation are presented. As a result, the experiment demonstrates that the proposed method is applicable to retrieve wave information based on the synthesized radar image. And, the proposed SWT-based method has better performance than that of the 3D FFT-based method and the CWT-based method for retrieving significant wave height.

Although the proposed retrieving method based on the SWT has good performance for retrieving the sea wave height, the effectiveness is still needed to further verify based on the collected X-band marine radar images in various sea conditions. Based on the SWT theory and the derivation, the estimated wavenumber should be a real number and can be accurately calculated. However, the estimated wavenumber is a complex number and exists an error since the effect of the shadowing and tilt modulation on the simulated radar images. Therefore, a similarity measure may be used to improve the estimation accuracy of the wavenumber. Besides, since the effect of the surface current on the retrieving accuracy of wave parameters is ignore in the CWT and the SWT methods, a bandpass filter for extracting wave spectrum from the wavenumber image spectrum from a single radar image is required for improving the application in practice. Compared with the traditional 3D FFT-based spectral analysis method, both the CWT and the SWT have the disadvantages of consuming large computer resource and are time-consuming. In the future, the spectral analysis method based on the fast WT is required.

REFERENCES

[1] M. T. Silva, R. Shahidi, E. W. Gill, and W. Huang, "Nonlinear extraction of directional ocean wave spectrum from bistatic HFSWR data," *IEEE J. Ocean. Eng.*, vol. 45, no. 3, pp. 1004–1021, May 2020.

[2] Z. Chen, B. Zhang, V. Kudryavtsev, Y. He, and X. Chu, "Estimation of sea surface current from X-band marine radar images by cross-spectrum analysis," *Remote Sens.*, vol. 11, no. 9, p. 1031, Apr. 2019.

[3] W. Huang, X. Liu, and E. Gill, "Ocean wind and wave measurements using X-band marine radar: A comprehensive review," *Remote Sens.*, vol. 9, no. 12, p. 1261, Dec. 2017.

[4] W. Duan, K. Yang, L. Huang, and X. Ma, "Numerical investigations on wave remote sensing from synthetic X-band radar sea clutter images by using deep convolutional neural networks," *Remote Sens.*, vol. 12, no. 7, p. 1117, Apr. 2020.

[5] W. Navarro, J. C. Velez, A. Orfila, and S. Lonin, "A shadowing mitigation approach for sea state parameters estimation using X-band remotely sensing radar data in coastal areas," *IEEE Trans. Geosci. Remote Sens.*, vol. 57, no. 9, pp. 6292–6310, Sep. 2019.

[6] Z. Chen, X. Chen, C. Zhao, and Z. Wang, "Wave height and wave period derived from a shipboard coherent S-band wave radar in the south China sea," *Remote Sens.*, vol. 11, no. 23, p. 2812, Nov. 2019.

[7] R. Gangeskar, "An algorithm for estimation of wave height from shadowing in X-band radar sea surface images," *IEEE Trans. Geosci. Remote Sens.*, vol. 52, no. 6, pp. 3373–3381, Jun. 2014.
[8] Y. Wei, Z. Lu, G. Pian, and H. Liu, "Wave height estimation from shadowing based on the acquired X-band marine radar images in coastal area," *Remote Sens.*, vol. 9, no. 8, p. 859, Aug. 2017.
[9] S. Salcedo-Sanz, J. C. Nieto Borge, L. Carro-Calvo, L. Cuadra, K. Hessner, and E. Alexandre, "Significant wave height estimation using SVR algorithms and shadowing information from simulated and real measured X-band radar images of the sea surface," *Ocean Eng.*, vol. 101, pp. 244–253, Jun. 2015.
[10] X. Chen, W. Huang, C. Zhao, and Y. Tian, "Rain detection from X-band marine radar images: A support vector machine-based approach," *IEEE Trans. Geosci. Remote Sens.*, vol. 58, no. 3, pp. 2115–2123, Mar. 2020.
[11] X. Chen and W. Huang, "Identification of rain and low-backscatter regions in X-band marine radar images: An unsupervised approach," *IEEE Trans. Geosci. Remote Sens.*, vol. 58, no. 6, pp. 4225–4236, Jun. 2020.
[12] H. Dankert, J. Horstmann, and W. Rosenthal, "Wind- and wave-field measurements using marine X-band radar-image sequences," *IEEE J. Ocean. Eng.*, vol. 30, no. 3, pp. 534–542, Jul. 2005.
[13] J. C. Nieto-Borge, P. Jarabo-Amores, D. de la Mata-Moya, and K. Hessner, "Signal-to-noise ratio analysis to estimate ocean wave heights from X-band marine radar image time series," *IET Radar, Sonar Navigat.*, vol. 2, no. 1, pp. 35–41, Feb. 2008.
[14] Z. Chen, B. Zhang, Y. He, Z. Qiu, and W. Perrie, "A new modulation transfer function for ocean wave spectra retrieval from X-band marine radar imagery," *Chin. J. Oceanol. Limnology*, vol. 33, no. 5, pp. 1132–1141, Jan. 2015.
[15] B. Lund, C. O. Collins, H. C. Graber, E. Terrill, and T. H. C. Herbers, "Marine radar ocean wave retrieval's dependency on range and azimuth," *Ocean Dyn.*, vol. 64, no. 7, pp. 999–1018, Jun. 2014.
[16] D.-J. Doong, L.-C. Wu, and J.-W. Lai, "Determination of the spatial pattern of wave directions in the inhomogeneous coastal ocean by marine radar image sequences," *IEEE Access*, vol. 6, pp. 45762–45771, 2018.
[17] L. Chuang, L.-C. Wu, and J.-H. Wang, "Continuous wavelet transform analysis of acceleration signals measured from a wave buoy," *Sensors*, vol. 13, no. 8, pp. 10908–10930, Aug. 2013.
[18] D. Jordan, R. W. Miksad, and E. J. Powers, "Implementation of the continuous wavelet transform for digital time series analysis," *Rev. Sci. Instrum.*, vol. 68, no. 3, pp. 1484–1494, Mar. 1997.
[19] G. Zha, Q. He, C. Guan, and J. Chen, "A curvelet-based method to determine wave directions from nautical X-band radar images," *Acta Oceanol. Sinica*, vol. 37, no. 1, pp. 11–19, Jan. 2018.
[20] L. Z.-H. Chuang, L.-C. Wu, D.-J. Doong, and C. C. Kao, "Two-dimensional continuous wavelet transform of simulated spatial images of waves on a slowly varying topography," *Ocean Eng.*, vol. 35, no. 10, pp. 1039–1051, Jul. 2008.
[21] L. Z.-H. Chuang and L.-C. Wu, "Study of wave group velocity estimation from inhomogeneous sea-surface image sequences by spatiotemporal continuous wavelet transform," *IEEE J. Ocean. Eng.*, vol. 39, no. 3, pp. 444–457, Jul. 2014.
[22] L. C. Wu, L. Z. H. Chuang, D. J. Doong, and C. C. Kao, "Ocean remotely sensed image analysis using two-dimensional continuous wavelet transforms," *Int. J. Remote Sens.*, vol. 32, no. 23, pp. 8779–8798, Aug. 2011.
[23] J. An, W. Huang, and E. Gill, "2-D continuous wavelet-based algorithm for extracting wave information from nautical radar images," in *Proc. IEEE Radar Conf. (RadarCon13)*, Ottawa, ON, Canada, Apr. 2013.
[24] J. An, W. Huang, and E. W. Gill, "A self-adaptive wavelet-based algorithm for wave measurement using nautical radar," *IEEE Trans. Geosci. Remote Sens.*, vol. 53, no. 1, pp. 567–577, Jan. 2015.
[25] P. Chernyshov, T. Vrecica, M. Streßer, R. Carrasco, and Y. Toledo, "Rapid wavelet-based bathymetry inversion method for nearshore X-band radars," *Remote Sens. Environ.*, vol. 240, Apr. 2020, Art. no. 111688.
[26] I. Daubechies, "A nonlinear squeezing of the continuous wavelet transform based on auditory nerve models," in *Wavelets in Medicine and Biology*, A. Aldroubi, and M. Unser, Eds. Boca Raton, FL, USA: CRC Press, 1996, pp. 527–546.
[27] I. Daubechies, J. Lu, and H.-T. Wu, "Synchrosqueezed wavelet transforms: An empirical mode decomposition-like tool," *Appl. Comput. Harmon. Anal.*, vol. 30, no. 2, pp. 243–261, Mar. 2011.
[28] H. Yang, J. Lu, and L. Ying, "Crystal image analysis using 2D synchrosqueezed transforms," *Multiscale Model. Simul.*, vol. 13, no. 4, pp. 1542–1572, Jan. 2015.
[29] J. C. Nieto-Borge, G. R. Rodiguez, and K. Hessner, "Inversion of marine radar images for surface wave analysis," *J. Atmos. Ocean. Technol.*, vol. 21, no. 8, pp. 1291–1301, Aug. 2004.
[30] I. R. Young, W. Rosenthal, and F. Ziemer, "A three-dimensional analysis of marine radar images for the determination of ocean wave directionality and surface currents," *J. Geophys. Res.*, vol. 90, no. C1, pp. 1049–1059, Jan. 1985.

YANBO WEI received the B.Sc. degree from the Anyang Institute of Technology, in 2011, and the Ph.D. degree from Harbin Engineering University, in 2017. From 2014 to 2016, he was with the Department of Electronic and Computer Engineering, McMaster University, as a Visiting Student. He is currently a Lecturer with the College of Physical and Electronic Information, Luoyang Normal University. His main research interest includes retrieving wave information from X-band marine radar images.

YAN ZHENG received the B.Eng. degree in electronic engineering from the Changchun University of Science and Technology of China, in 2010, and the M.Sc. degree from Harbin Engineering University, in 2014. He is currently pursuing the Ph.D. degree. His research interests include marine radar image processing and analysis and computer software engineering.

ZHIZHONG LU received the B.Sc. degree from Fudan University, in 1989, and the M.Sc. and Ph.D. degrees from Harbin Engineering University, in 2001 and 2008, respectively. He is currently a Professor with the College of Automation, Harbin Engineering University. His main research interests include marine integrated hydrological remote sensing and information forecasting technology.